

Solution NMR Determination of the Seating(s) of Meso-nitro-etioheme-1 in Myoglobin: Implications for Steric Constraints to Meso Position Access in Heme Degradation by Coupled Oxidation

Jingtao Wang, Yiming Li, Dejian Ma, Heather Kalish, Alan L. Balch, and Gerd N. La Mar*

Contribution from the Department of Chemistry, University of California, Davis, California 95616

Received March 12, 2001. Revised Manuscript Received June 15, 2001

Abstract: The highly stereoselective cleavage of hemin in myoglobin by coupled oxidation has been attributed to steric barriers that leave more space near the α - than the other meso-positions. The steric barriers near meso positions in myoglobin have been investigated by establishing the thermodynamics and dynamics of possible seatings in the pocket of horse myoglobin of a four-fold symmetric etioheme I modified with a bulky nitro group at a single meso position. The cyanomet complex of this reconstituted myoglobin exhibits three sets of ^1H NMR resonances that are linked dynamically and occur in approximate populations ratios of 0.82:0.10:0.08. Two dimensional ^1H NMR has been used to assign the hemin and heme pocket resonances in the major isomer in solution and to determine that the hemin is oriented with the nitro group at the canonical γ -meso position of native hemin. The dominance of this isomer is attributed to the solvent exposure of this portion of the hemin which stabilizes the highly polar nitro group. Using a combination of magnetization transfer among methyl groups of the three isomers due to “hopping” of the hemin about its normal, the assigned resonances of an isoelectronic, bis-cyano complex of meso-nitro-etioheme I, and the known essentially constant rhombic perturbation of heme pocket sites on the hyperfine shifts of heme methyl (Kolczak, U.; Hauksson, J. B.; Davis, N. L.; Pande, U.; de Ropp, J. S.; Langry, K. C.; Smith, K. M.; LaMar, G. N. *J. Am. Chem. Soc.* **1999**, *121*, 835–843); the two minor isomers are shown to place their bulky nitro group at the canonical δ -meso (8%) and α -meso positions (10%). The comparable population of the isomers with nitro groups at the hydrophobic α - and δ -meso positions dictates that, while the static crystal structure finds more room near the α -meso position, the deformation at minimal energetic expense near the α - and δ -meso positions is comparable. These results argue that factors other than simple steric influences control the selectivity of the ring cleavage in myoglobin.

Introduction

The biological degradation of heme is carried out by the enzyme heme oxygenase, HO,¹ which excises the meso carbon at solely the α -meso position of native protoheme (1) to yield α -biliverdin and CO in its dual role in the catabolism of heme² and the generation of a putative neural messenger,³ CO. This reaction can be modeled in vitro by degrading heme to yield a mixture of verdoheme, biliverdin and its iron complex, and CO, using dioxygen as oxidant in the presence of a reducing agent^{4–6} (ascorbic acid or hydrazine) (coupled oxidation). For the free

hemin, the four meso bridges are equally susceptible to excision by coupled oxidation⁷ and only slightly differentiated when reacted with hydrogen peroxide.⁸ When the coupled oxidation is carried out in a heme protein such as myoglobin,⁹ Mb, or cytochrome *b*₅,^{10,11} the heme is again similarly cleaved, with a strong preference (95%) for the α -meso position. Both electronic and steric influences have been invoked to rationalize the stereoselection of the heme ring opening^{12–16} in both HO and Mb. The stereoselectivity in Mb has been rationalized¹² on the

* Address correspondence to: Dr. Gerd N. La Mar, Department of Chemistry, University of California, Davis, CA 95616. Telephone: (530) 752-0958. Fax: (530) 752-8995. E-mail: lamar@indigo.ucdavis.edu.

(1) Abbreviations used: Mb, myoglobin; 2D, two-dimensional; TOCSY, 2D ^1H NMR correlation spectroscopy; DSS, 2,2-dimethyl-2-silapentane-5-sulfonate; HO, heme oxygenase; metMbCN, cyanometmyoglobin; metMb(x)CN, cyanometmyoglobin reconstituted with hemin x; COSY, correlation spectroscopy; NOESY, nuclear Overhauser spectroscopy; NOE, nuclear Overhauser effect; EXSY, 2D ^1H NMR exchange spectroscopy.

(2) Tenhunen, R.; Marver, H. S.; Schmid, R. *J. Biol. Chem.* **1969**, *244*, 6388–6394.

(3) Verma, A.; Hirsch, D. J.; Glatt, C. E.; Ronnett, G. V.; Snyder, S. H. *Science* **1993**, *259*, 381–384.

(4) Balch, A. L.; Latos-Grazynski, L.; Noll, B. C.; Olmstead, M. M.; Sztrenberg, L.; Safari, N. *J. Am. Chem. Soc.* **1993**, *115*, 1422–1429.

(5) Balch, A. L.; Latos-Grazynski, L.; Noll, B. C.; Olmstead, M. M.; Safari, N. *J. Am. Chem. Soc.* **1993**, *115*, 9056–9061.

(6) St. Claire, T. N.; Balch, A. L. *Inorg. Chem.* **1999**, *38*, 684–691.

(7) Bonnett, R.; McDonough, A. F. *J. Chem. Soc., Perkin Trans. 1* **1973**, *1*, 881–888.

(8) Kalish, H. R.; Latos-Grazynski, L.; Balch, A. L. *J. Am. Chem. Soc.* **2000**, *122*, 12478–12486.

(9) Hildebrand, D. P.; Tang, H.; Luo, Y.; Hunter, C. L.; Smith, M.; Brayer, G. D.; Mauk, A. G. *J. Am. Chem. Soc.* **1996**, *118*, 12909–12915.

(10) Rodriguez, J. C.; Rivera, M. *Biochemistry* **1998**, *37*, 13082–13090.

(11) Avila, L.; Huang, H.; Rodriguez, J. C.; Moënne-Loccoz, P.; Rivera, M. *J. Am. Chem. Soc.* **2000**, *122*, 7618–7619.

(12) Brown, S. B.; Chabot, A. A.; Enderby, E. A.; Nort, A. C. T. *Nature* **1981**, *289*, 93–95.

(13) Torpey, J.; Ortiz de Montellano, P. R. *J. Biol. Chem.* **1996**, *271*, 26067–26073.

(14) Torpey, J.; Ortiz de Montellano, P. R. *J. Biol. Chem.* **1997**, *272*, 22008–22014.

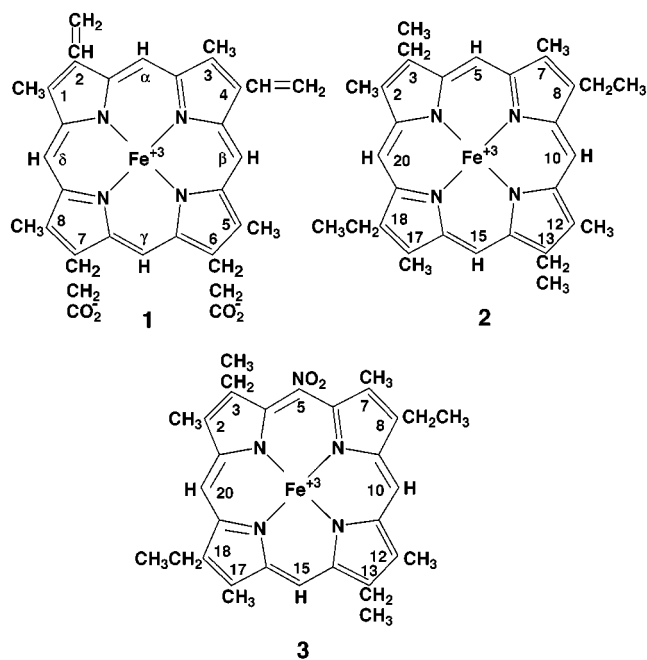
(15) Gorst, C. M.; Wilks, A.; Yeh, D. C.; Ortiz de Montellano, P. R.; La Mar, G. N. *J. Am. Chem. Soc.* **1998**, *120*, 8875–8884.

(16) Takahashi, S.; Ishikawa, K.; Takeuchi, N.; Ikeda-Saito, M.; Yoshida, T.; Rousseau, D. L. *J. Am. Chem. Soc.* **1995**, *117*, 6002–6006.

basis of a steric argument that finds more "space" near the α -meso than near the β -, γ -, or δ -meso-positions in Mb.

The recent solution of the HO crystal structure^{17,18} has shown that, in fact, the distal helix is closer to the heme than in other heme proteins and that the helix does sterically block all but the α -meso positions. However, the steric access to the β -, γ -, and δ -meso positions in HO-hemin complex is exerted directly by the relatively inflexible helix backbone,^{17,18} while the available access to the same meso position in myoglobin^{12,19} is determined primarily by the positions of side chain atoms. Since side chains may have considerable mobility, the static structure seen by X-ray crystallography does not necessarily reveal the deformability of the ground-state structure that could be functionally relevant for stereoselection in heme catabolism by coupled oxidation in myoglobin.

Recent studies of the influences of mutagenesis of Mb on heme cleavage by coupled oxidation have also suggested more complex factors are at work than simple steric effects in controlling stereospecificity of the cleavage.²⁰ Hence, we have initiated a study of the preferential deformability of the heme pocket in the vicinity of the four canonical meso positions of Mb. These studies utilize a four-fold symmetric heme such as etioheme I (**2**) for which the steric requirements of each of the four meso environments, as well as for the four pyrrole environments, are identical, such that the protein can distinguish only the alternate seating about a N-Fe-N axis (clockwise ethyl-methyl or counterclockwise ethyl-methyl when viewed from a given side of the heme). Solution ¹H NMR characteriza-



tion has already shown only that one of the orientations,²¹ that shown in Figure 1, is detectable in solution. When a single, bulky substituent such as a nitro group is introduced into etioheme I at one meso-position to yield meso-NO₂-etiohemin

(17) Schuller, D. J.; Wilks, A.; Ortiz de Montellano, P. R.; Poulos, T. L. *Nature Struct. Biol.* **1999**, *6*, 860–867.

(18) Sugishima, M.; Omata, Y.; Kakuta, Y.; Sakamoto, H.; Noguchi, M.; Fukuyama, K. *FEBS Lett.* **2000**, *471*, 61–66.

(19) Kuriyan, J.; Wilz, S.; Karplus, M.; Petsko, G. A. *J. Mol. Biol.* **1986**, *192*, 133–154.

(20) Murakami, T.; Morishima, I.; Matsui, T.; Ozaki, S.; Hara, I.; Yang, H.-J.; Watanabe, Y. *J. Am. Chem. Soc.* **1999**, *121*, 2007–2011.

(21) Tran, A.-T.; Kalish, H.; Balch, A. L.; La Mar, G. N. *J. Biol. Inorg. Chem.* **2000**, *5*, 624–633.

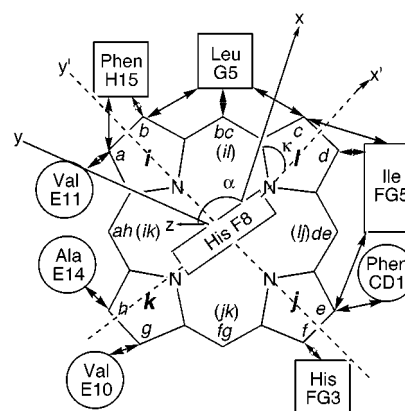


Figure 1. Schematic representation of the heme pocket of myoglobin showing the positions of important proximal (rectangles) and distal (circles) residues. The arrows connecting these residues to the heme and to each other reflect the expected, and observed, dipolar contacts. The heme positions are defined on a protein-based labeling scheme with the positions *a*–*h* representing the positions occupied by substituent at positions 1–8 for native protohemin. The individual pyrrole rings are arbitrarily labeled *i*, *j*, *k*, *l*, and the positions of these pyrrole rings for the major isomer of meso-NO₂-etiohemin I in metMbcN are shown.

I, **3**, the questions that arise are: where in the Mb heme pocket is this bulky substituent most readily accommodated and by what thermodynamic preference(s) over the alternate position(s)? The nitro group, which is constrained to lie perpendicular to the heme plane,²² is an effective probe of the space immediately adjacent to and above and below the reactive meso sites within the porphyrin.

The seatings of the heme are readily established by one direct and one indirect solution NMR approach. On one hand, the assignment by 1D/2D NMR of the complete meso-NO₂-etioheme I and the key heme pocket residues that line the pocket, followed by establishing the proximity of the individual heme substituents to the individual residues within the protein matrix, lead to the unique seating of the heme.^{21,23,24} This approach demands the unambiguous location and assignment of the three remaining meso-H's to place the NO₂ in the heme pocket. The assignment of meso-H's is particularly disadvantageous in metMbcN, since the protons do not yield resolved signals and are the most strongly relaxed of the heme protons.^{25,26} On the other hand, an alternate route to establishing the heme orientation makes use of a previous study which showed that reconstituting a heme which is rhombically perturbed by chemical substitution into metMbcN results in chemical shifts that are the vector sum of the shifts in the model compound^{27,28} and the rhombic influences, for each position of the heme, imposed by the protein matrix.²⁹ Thus, the influence of the metMbcN pocket can be represented by the *change* in chemical shift that the different positions in the protein matrix induce for a methyl group from

(22) Senge, M. O.; Eigenbrot, C. W.; Brennan, T. D.; Shusta, J.; Scheidt, W. R.; Smith, K. M. *Inorg. Chem.* **1993**, *32*, 3134–3142.

(23) Hauksson, J. B.; La Mar, G. N.; Pandey, R. K.; Rezzano, I. N.; Smith, K. M. *J. Am. Chem. Soc.* **1990**, *112*, 6198–6205.

(24) Hauksson, J. B.; La Mar, G. N.; Pandey, R. K.; Rezzano, I. N.; Smith, K. M. *J. Am. Chem. Soc.* **1990**, *112*, 8315–8323.

(25) Emerson, S. D.; La Mar, G. N. *Biochemistry* **1990**, *29*, 1556–1566.

(26) Qin, J.; La Mar, G. N. *J. Biomol. NMR* **1992**, *2*, 597–618.

(27) La Mar, G. N.; Viscio, D. B.; Smith, K. M.; Caughey, W. S.; Smith, M. L. *J. Am. Chem. Soc.* **1978**, *100*, 8085–8092.

(28) La Mar, G. N.; Budd, D. L.; Viscio, D. B.; Smith, K. M.; Langry, K. C. *Proc. Natl. Acad. Sci., U.S.A.* **1978**, *75*, 5755–5759.

(29) Kolczak, U.; Hauksson, J. B.; Davis, N. L.; Pande, U.; de Ropp, J. S.; Langry, K. C.; Smith, K. M.; La Mar, G. N. *J. Am. Chem. Soc.* **1999**, *121*, 835–843.

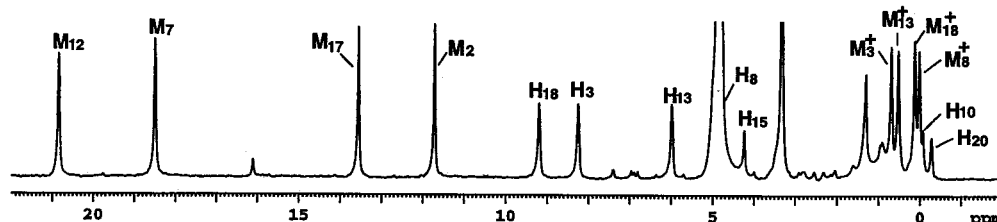


Figure 2. 400 MHz ^1H NMR spectrum of the model compound bis-cyano-meso-nitro-etiohemin I, [hemin **3**](CN) $_2^{-1}$, in methanol at 25 °C. The resonances assigned by 2D NMR are labeled by the conventional numbering scheme shown in structure **3**.

that in the model compound.²⁹ This latter approach requires the assignment of the ^1H NMR spectrum for the isoelectronic model compound^{27,28} in the form of the bis-cyano complex of ferric meso-NO $_2$ etioheme I.

We present herein the results of our study of the incorporation of meso-nitro-etioheme I into horse metMbCN that demonstrates that, in fact, the nitro-group can be accommodated detectably at all canonical meso positions except the β -meso position of native protohemin, with the stronger preference for the γ -, but significant and comparable populations of the nitro group at the α - and δ -meso positions.

Experimental Section

Synthesis of Meso-nitro-etioheme I. Meso-nitro-etioheme I (**3**) was obtained by the nitration of etioporphyrin I with fuming nitric acid using the procedure developed for octaethylporphyrin³⁰ and insertion of iron by boiling the nitrated porphyrin with FeCl $_2 \cdot 4\text{H}_2\text{O}$ in dimethylformamide. Bis-cyanonitro-etioheme I complex (2 mM), designated [hemin **3**](CN) $_2^{-1}$, was prepared by dissolving **3** in 0.5 mL of (C $_2\text{H}_5$) $_2$ SO: $^2\text{H}_2\text{O}$ 1:2 vol:vol or pure C $_2\text{H}_5\text{O}^2\text{H}$ in the presence of 10-fold molar excess of KCN. The sample was used for ^1H 2D COSY and NOESY experiments.

Reconstitution of Myoglobin. Horse skeletal myoglobin (Mb) was purchased from Sigma Chemical Co. as a lyophilized powder and used without further purification. Apomyoglobin (apoMb) was prepared according to standard procedures³¹ by using 0.1 N HCl to dissociate heme from myoglobin and separating the heme by extraction with methylethyl ketone, as described previously.^{21,23,24} Reconstitution of meso-nitro-etioheme I, **3**, into myoglobin was carried out by adding 1.2 mol equiv of [hemin **3**](CN) $_2^{-1}$ solution dropwise into 20 mL of 0.27 mM apoMb buffered with 0.1 M potassium phosphate at pH 7.0 in an ice bath. After addition, the solution was stirred for 20 min. The solution was loaded on a Sephadex G-25 column to remove the organic solvent. The column was eluted with 0.1 M phosphate buffer at pH 7.0. The yield of the reconstituted Mb was $\sim 80\%$. Subsequently, the solution was concentrated by ultrafiltration (Amicon) and the solvent replaced with 0.1 M potassium phosphate buffer in $^2\text{H}_2\text{O}$ at pH 7.0 containing 20 mM KCN. The resulting cyanomet complex of meso-nitro-etioheme I is abbreviated metMb(**3**)CN.

NMR Spectroscopy. ^1H NMR spectra were recorded on either a Varian INOVA 400 (model complex) or a Bruker AVANCE 600 (protein complex) spectrometer operating at 400 and 600 MHz, respectively. Reference spectra over a range of temperatures were collected over a 24.0 kHz (400 MHz) and 42.0 kHz (600 MHz) bandwidth under nonsaturating conditions (1 s $^{-1}$). The T_1 's were determined by the standard inversion–recovery experiment at 400 MHz (model complex) and 600 MHz (protein complex). The 1D spectra were exponentially apodized with 1 Hz (model complex) or 5 Hz (protein complex) line broadening. COSY³² spectra at 25 °C were determined for the model complex at 400 MHz over a 12 kHz bandwidth with 256 t_1 blocks of 128 scans and 2048 t_2 points collected at a repetition rate of 1 s $^{-1}$. NOESY³³ spectra (50 ms mixing times) at -20 °C were

Table 1. Chemical Shifts of the Bis-cyano Complex of Meso-nitro-etiohemin I

label ^a	$\delta_{\text{DSS}}(\text{obs})^b$	label ^a	$\delta_{\text{DSS}}(\text{obs})^b$
M $_2$	11.70	H $_{13\alpha}$	5.97
H $_{3\alpha}$	8.25	M $^+_{13\beta}$	0.52
M $^+_{3\beta}$	0.69	H $_{15}$	4.22
M $_7$	18.49	M $_{17}$	13.54
H $_{8\alpha}$	4.74	H $_{18\alpha}$	9.18
M $^+_{8\beta}$	0.01	M $^+_{8\beta}$	0.12
H $_{10}$	-0.08	H $_{20}$	-0.29
M $_{12}$	20.85		

^a M $_q$ is core methyl and H $_q$'s and M ^+_q are ethyl group methylene and terminal methyl groups, respectively, where q is one of the positions as labeled in **3**. ^b Shifts, in ppm from DSS, in C $_2\text{H}_5\text{O}^2\text{H}$ solution at 25 °C.

determined for the model complex at 400 MHz over a 16.0 kHz bandwidth with 512 t_1 blocks of 96 scans each and 2048 t_2 points collected as a repetition rate of 3 s $^{-1}$. TOCSY spectra³⁴ (30 ms mixing times) at 25 °C and NOESY/EXSY spectra³³ (60 ms mixing time) at 5° intervals between 5° and 30 °C were recorded at 600 MHz over a 30 kHz bandwidth using 512 t_1 blocks of 256 scans each and 2048 t_2 points at a repetition rate of 2 s $^{-1}$. The 2D data sets were apodized by 30°-shifted-sine-bell-squared function and zero-filled to 2048 \times 2048 points prior to Fourier transformation.

Results

Assignment of Bis-cyano-meso-nitro-etioheme I. The 400 MHz ^1H NMR spectrum of the model complex in C $_2\text{H}_5\text{O}^2\text{H}$ is illustrated in Figure 2. Peaks are labeled M $_i$ (core methyl), H $_i$ (core methylene protons), and M ^+_i (terminal methyls) where i is the position as labeled in **3**. COSY spectra at 25 °C reveal the spin connectivity of the four ethyl groups (not shown, see Supporting Information). NOESY spectra in 2:1 vol:vol (C $_2\text{H}_5$) $_2$ SO: $^2\text{H}_2\text{O}$ at -20 °C (not shown, see Supporting Information), where solvent viscosity is sufficiently high to yield strong cross-peaks,³⁵ lead to the necessary dipolar connections about the hemin, which include the three strongly relaxed meso-H's, and hence provide unambiguous assignment of all 15 expected signals, as listed for the same complex in methanol in Table 1, using the labeling scheme depicted in **3**.

Temperature Effects on NMR Spectra of Metmb(NO $_2$ -etio)CN Hemin. The 600 MHz ^1H NMR spectra of the protein complex in $^2\text{H}_2\text{O}$ as a function of temperature are illustrated in Figure 3. The major species has apparent methyl and single proton peaks labeled M $_q$, and H $_q$, respectively (where q defines a particular pyrrole ring of the hemin). However, a large number of peaks with intensities less than one proton for the major isomer are observed. These minor component peaks can be

(33) Jeener, J.; Meier, B. H.; Bachmann, P.; Ernst, R. R. *J. Chem. Phys.* **1979**, *71*, 4546–4553.

(34) Griesinger, C.; Otting, G.; Wüthrich, K.; Ernst, R. R. *J. Am. Chem. Soc.* **1988**, *110*, 7870–7872.

(35) Licocchia, S.; Chatfield, M. J.; La Mar, G. N.; Smith, K. M.; Mansfield, K. E.; Anderson, R. R. *J. Am. Chem. Soc.* **1989**, *111*, 6087–6093.

(30) Bonnett, R.; Stephenson, G. F. *J. Org. Chem.* **1965**, *30*, 2791–2799.

(31) Teale, F. W. J. *Biochim. Biophys. Acta* **1959**, *35*, 543.

(32) Bax, A. *Two-Dimensional Nuclear Magnetic Resonance in Liquids*; D. Reidel Publishing Company: Dordrecht, Holland, 1982.

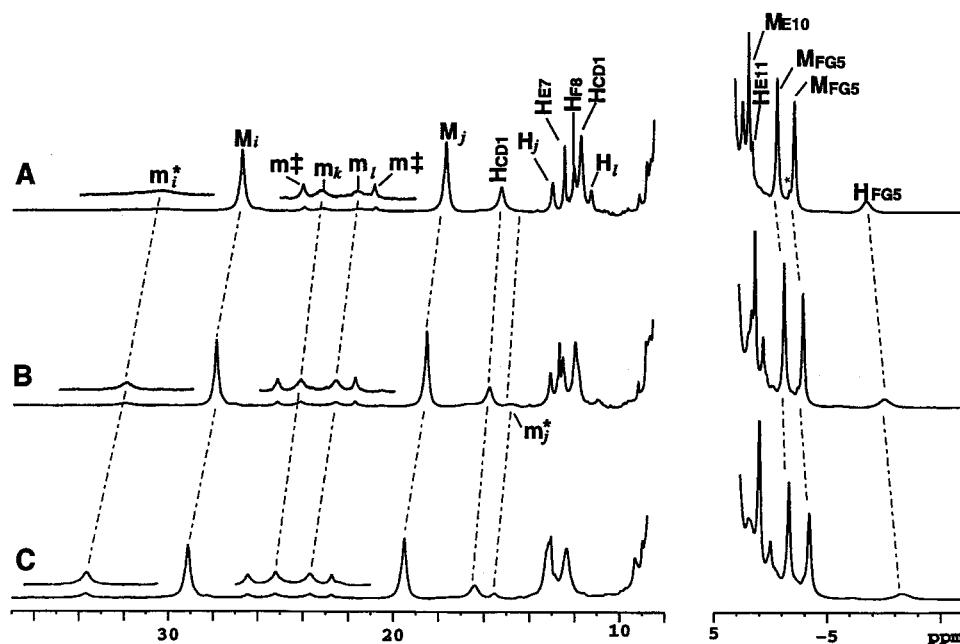


Figure 3. Resolved portions of the 600 MHz ^1H NMR spectra of ~ 3 mM metMb(3)CN in $^2\text{H}_2\text{O}$ 50 mM phosphate, 10 mM KCN at pH 8.2 at: (A) 25 $^\circ\text{C}$; (B) 15 $^\circ\text{C}$; and (C) 5 $^\circ\text{C}$. The resonances for methyls and single protons for the major isomer in solution are labeled M_q , H_q , respectively, where $q = i, j, k, l$ for the pyrrole ring methyl or methylene protons, or $q =$ helical or interhelical position of the residue. The same sets of peaks in two different minor isomers are similarly labeled either m_q , h_q or m^*_q , h^*_q . Two resolved methyl peaks for some unreacted etioheme-I complexes are labeled by m^\ddagger .

attributed to three additional distinct species, where two of them represent alternate isomers of the species with peaks M_q , H_q , and the peaks marked m^\ddagger arise from methyls from the unreacted etioheme I impurity.²¹ The remaining peaks are labeled m_q , h_q for one minor isomer, and m^*_q , h^*_q for the other minor isomer of the protein complex of interest. As the temperature is lowered, the peaks for the two minor isomers become narrower, indicating that exchange among two or more of the isomers is responsible for the line broadening at higher temperatures.³⁶ At 10 $^\circ\text{C}$, integration differentiates the intensities of m^* and m , which, upon comparison to the intensity of M_i , leads to a population $M_i:m^*_i:m_i \sim 0.82:0.10:0.08$. The lifetimes³⁶ of the minor species are on the order of 1 ms and that for the major species is ~ 10 ms at 25 $^\circ\text{C}$.

Labeling of Meso-nitroetioheme Resonances. The unambiguous definition of the seating(s) of the heme can be effectively carried out only on the major isomer, and the nature of minor isomers must be established on the basis of how the environment of a given methyl on the heme is altered upon converting the major into one of the minor isomers. Hence, initially, a heme-based labeling of substituents is required. First, we arbitrarily label the four pyrrole rings as i, j, k , and l each of which have one core, methyl, M_q , two $\alpha\text{-CH}'\text{s}$, H_q' 's, and a terminal methyl M^+_q for $q = i, j, k, l$. Thus, the two resolved methyls in Figure 3 are labeled M_i and M_j . These pyrrole rings, i, j, k , and l , must next be positioned relative to each other, and the position of each core methyl or ethyl group in the protein matrix must be determined. The positions within the *protein matrix* are defined by the subscripts, $a-h$, as shown in Figure 1, which correspond to the canonical 1–8 positions of native protohemin. *The definitive seating of the heme is subsequently established by the position at which meso-H's can be located.* It is solely the location of the meso-H's that, by inference, identifies the location of the nitro group. The methyl resonances for the two minor isomers are initially labeled solely by the

index of the pyrrole of the major component with which there will be shown to be exchange. This leads to labeling m_k and m_l as well as m_i^* and m_j^* in Figure 3.

Exchange Behavior among Isomers for the Heme Methyls.

The NOESY slices through major isomer methyl peaks M_i and M_j reveal temperature-dependent magnetization transfer³⁶ to two additional peaks, each labeled m^*_i , m^*_j for the species with extreme low-field shifts, and labeled m_i , m_j for the isomers with shifts in the 5–10 ppm spectral window, as shown in Figure 4, B and C, respectively. The slices through the minor component peaks m_k and m_l reveal large magnetization-transfer peaks to two unresolved signals in the diamagnetic envelope (not shown). However, when NOESY slices through these two latter frequencies, labeled M_k , M_l , are inspected at the same scale as the slices through resolved M_i and M_j , they exhibit magnetization transfer to two sets of peaks, the resolved low-field m_k and m_l , and peaks labeled m^*_i and m^*_j in the 5–10 ppm window, as shown in Figure 4, D and E, respectively, with intensities (at all temperatures) comparable to that revealed by peaks m_q , m^*_q in Figure 4, B and C. These data locate each of the four methyl peaks from the three detectable, interconverting species, and the same data over a range of temperatures yield the Curie plots for all methyls for the three species, as illustrated in Figure 5.

Assignment of Heme Pocket Residues in the Major Isomer. The key heme pocket residues for seating the heme^{21,23,24} and locating magnetic axes,²⁵ Phe 43(CD1), His64(E7), Val67-(E10), Val68(E11), Ala71(E14), Leu89(F4), Ala90(F5), His93-(F8), His97(FG3), Ile99(FG5), Tyr104(G4), Leu105(G5), and Phe139(H15), are identified by spin-connectivity in TOCSY spectra and spatially placed relative to each other by dipolar contact in NOESY spectra in a standard fashion described in detail for both WT^{25,37,38} and numerous point mutants of metMbCN,^{39–42} as well as metMb(2)CN²¹ (data not shown).

(37) Rajarathnam, K.; La Mar, G. N.; Chiu, M. L.; Sligar, S. G. *J. Am. Chem. Soc.* **1992**, *114*, 9048–9058.

(38) Nguyen, B. D.; Xia, Z.; Yeh, D. C.; Vyas, K.; Deaguero, H.; La Mar, G. *J. Am. Chem. Soc.* **1999**, *121*, 208–217.

(36) Sandström, J. *Dynamic NMR Spectroscopy*; Academic Press: New York, 1982.

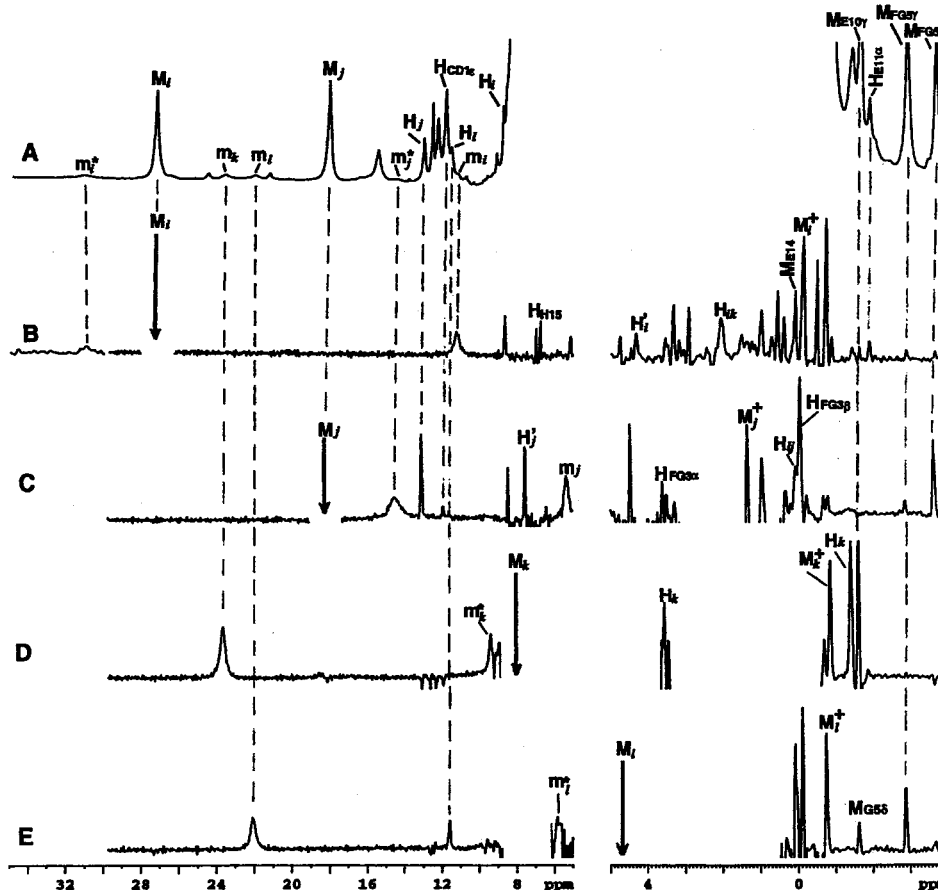


Figure 4. (A) 600 MHz ^1H NMR reference spectrum of ~ 3 mM metMb(3)CN in $^2\text{H}_2\text{O}$, 50 mM phosphate, 100 mM NaCl, 10 mM KCN, pH 8.2 at 20 $^\circ\text{C}$. NOESY slices at constant vertical scale through the major isomer heme methyls (B) M_i ; (C) M_j ; (D) M_k ; and (E) M_l . The position of the diagonal is shown by a vertical arrow. The peaks with strongly temperature-dependent magnetization transfer to minor isomer methyl peaks are labeled m_i or m_i^* . NOESY cross-peaks for the major isomer that locate pyrrole methylene protons, H_q , and to the meso- H 's (labeled $H_{q,q'}$, where q, q' are the two pyrroles bridged by the meso) and NOESY cross-peaks to key heme pocket residual protons allow unambiguous determination of the location of a methyl at one of positions $a-h$ are also labeled.

The observed contacts are depicted schematically in Figure 1. The T_1 's for the resolved peak for Phe43(CD1) ($T_1(\text{C}_\alpha\text{H}) \sim 20$ ms) and Ile99(FG5) ($T_1(\text{C}_\gamma\text{H}) \sim 60$ ms) were found to be unchanged from those in WT metMbCN.²⁵ The chemical shifts for these residues are listed in Supporting Information.

Assignment of Pyrrole Substituents. TOCSY spectra (not shown) of metMb(3)CN reveal three additional spin systems involving relaxed protons with significant dipolar shifts (as reflected in strongly temperature-dependent shifts), which must originate from the heme. These include three three-spin systems with resolved single protons in the low-field window and one with strongly upfield-shifted single protons. The third ethyl exhibits too large a dispersion for TOCSY detection but is readily identified by NOESY (see Supporting Information). Strong NOESY cross-peaks between each of the four core methyls, M_i-M_l , and one of the α -methylene protons of each ethyl group result in the unequivocal identification of all four signals for each of pyrrole $i-l$ (labeled in NOESY slices through the heme methyl in Figure 4). Weak NOESY cross-peaks between the core methylene of one pyrrole and one of the α -methyl protons of another pyrrole allow the unambiguous

assignment of the four pyrroles as lying clockwise $i \rightarrow l \rightarrow j \rightarrow k$ (as shown in Figure 1) but provide no information as to where the NO_2 group is located.

Assignment of Meso- H 's. Unambiguous assignment of meso- H 's is difficult, since they exhibit no TOCSY connectivity, are strongly relaxed, and generally go unresolved under the intense aliphatic spectral window. The available strategy for assignment involves the detection of weak-to-moderate intensity NOESY cross-peaks by the heme methyls to protons with strongly temperature-dependent shifts which exhibit unique intercepts (at $T \rightarrow \infty$) in the 10–20 ppm window in a Curie plot ($\delta_{\text{DSS}}(\text{obs})$) vs reciprocal absolute temperature).²⁶ The located meso- H 's will initially be labeled $H_{il}, H_{lj}, H_{jk}, H_{ik}$ to indicate the adjacent pyrrole rings they bridge.

The NOESY slices through methyls M_i and M_j in Figure 4, B and C, each exhibit a moderate intensity cross-peak to a proton with the characteristic temperature dependence (see Figure 5), identifying meso-protons H_{jk} and H_{ij} . The detection of similar NOESY cross-peaks for methyls M_k and M_l is problematic, since neither the methyl nor the expected meso- H is resolved. Moreover, the meso- H could be expected to have shifts similar to the methyl, making the resolution and detection of the desired cross-peaks very difficult in the crowded spectral window. Hence, we must postpone location and assignment of the last meso- H until we have placed each pyrrole substituent at one of the eight canonical pyrrole positions $a-h$ in the heme pocket (Figure 1).

(39) Rajarathnam, K.; Qin, J.; La Mar, G. N.; Chiu, M. L.; Sligar, S. G. *Biochemistry* **1993**, *32*, 5670–5680.

(40) Rajarathnam, K.; Qin, J.; La Mar, G. N.; Chiu, M. L.; Sligar, S. G. *Biochemistry* **1994**, *33*, 5493–5501.

(41) Qin, J.; La Mar, G. N.; Cutruzzolá, F.; Travaglini Allocatelli, C.; Brancaccio, A.; Brunori, M. *Biophys. J.* **1993**, *65*, 2178–2190.

(42) Wu, Y.; Chien, E. Y. T.; Sligar, S. G.; La Mar, G. N. *Biochemistry* **1998**, *37*, 6979–6990.

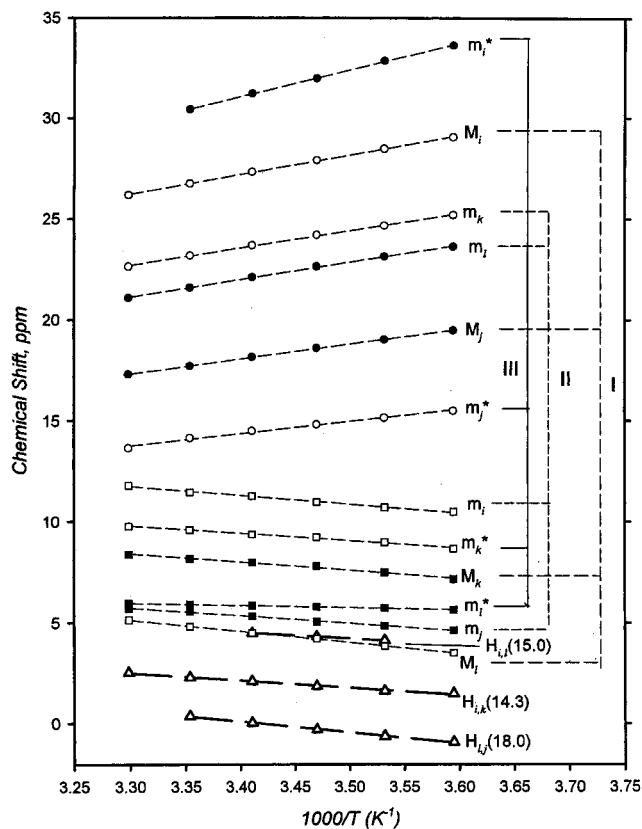


Figure 5. Curie plot ($\delta_{\text{DSS}}^{\text{obs}}$) versus reciprocal absolute temperature) for both meso-H's ($H_{q,q'}$) and heme methyls (M_q) of the major isomer, **I** in Figure 7, and the heme methyls of minor isomers **II** (m_q^* 's) and **III** (m_q^* 's) of metMb(3)CN. The methyls are identified by the positions (a, c, e, g) in the protein matrix a (open circles), c (open squares), e (closed circles), and g (closed squares). The meso-H's are shown by open triangles. The values in parentheses give the intercept, in ppm relative to DSS, of meso-H's.

Seating the Heme in the Major Isomer. The NOESY slices in Figure 4 for the four heme methyls, M_i – M_l , of metMb(3)CN exhibit NOEs to Phe43(CD1) $C_\alpha H$'s and Ile99(FG5) $C_\delta H_3$ (by M_j); Ile99(FG5) $C_\gamma H_3$ and Leu104(G5) $C_\delta H_3$ (by M_j); Val68(E11) $C_\alpha H$ and Ala71(E14) $C_\beta H_3$ (by M_i) and to Val67-(E10) $C_\gamma H_3$ (by M_k), which are essentially the same as observed²¹ for metMb(2)CN methyls at positions $a(1)$, $c(3)$, $e(5)$ and $g(7)$, respectively, as shown in Figure 1. Since H_i 's exhibit NOESY cross-peaks to Phe138(H15) and H_j 's display NOESY cross-peaks to the ring His93(FG3), the orientation of the tetrapyrrole is uniquely established to be that illustrated in Figure 1. This is the same orientation with respect to the positions of ethyls and methyls as previously deduced for unreacted etiohemine I.²¹

The pattern of NOESY cross-peaks to the heme pocket residues, together with the location of two of the three meso-H's, dictates an orientation in the heme pocket with methyls occupying positions $a(M_i)$, $c(M_l)$, $e(M_j)$, and $g(M_k)$, methylene protons occupying positions $b(H_i)$, $d(H_j)$, $f(H_k)$, $h(H_l)$, and protons at meso-positions de (lj) and ah (ik). Having located pyrrole rings i and l at the position shown in Figure 1, the presence of a meso-H at position H_{il} (or H_{bc}) is also approachable by the expected very strong NOESY cross-peak from the well upfield-shifted Leu104(G5) $C_\delta H_3$ (~ 2.5 Å between $C_\delta H_3$ and α -meso-H in MbCO).^{19,25} The portion of the NOESY map illustrating a cross-peak with Leu104(G5) $C_\delta H_3$ to a proton with the expected low-field intercept, is shown in Figure 6 and hence locates meso-proton H_{il} ($=H_{bc}$). The identification of the

three meso-H's adjacent to methyls i, j , and l dictates that the meso- NO_2 must be located between pyrrole rings j and k , that is, at position fg as shown in Figure 1. Hence, protons occupy meso positions bc (H_{il}), de (H_{lj}), and ha (H_{ik}) but not position fg (H_{jk}). The positions a – h correspond to the canonical positions 1–8, and $bc, de, ha,$ and fg are the same as the α -, β -, δ -, and γ -positions, respectively, of natural protohemin. Thus, the major isomer ($\sim 82\%$), corresponds to a right-handed methyl–ethyl arrangement of etiohemine I with the nitro group located at the usual γ -position. This orientation is shown Figure 1 and in structure **I** of Figure 7.

Prediction of Methyl Hyperfine Shifts. Previous detailed analysis of the ^1H NMR spectra of a large number of chemically modified hemins, both as bis-cyano model compounds and reconstituted into iso-electronic metMbCN, had shown that the protein adds a rhombic contribution to the heme methyl shift that is additive to that exerted by peripheral substituents and that the protein-based perturbation is in the form of an essentially invariant shift perturbation that is completely diagnostic of the protein environment occupied by positions a – h , in 1–8, in the heme pocket.²⁹ Thus, the predicted shift for methyl at position $r = a$ – h (in Figure 1) in metMb(3)CN, $\delta'_{\text{DSS}}(\text{pred, metMb(3)CN})$, is related to the observed shift in the model compound, $\delta_{\text{DSS}}(\text{obs, [hemin 3](CN)}_2^{-1})$ via:

$$\delta'_{\text{DSS}}(\text{pred, metMb(3)CN}) = \delta'_{\text{DSS}}(\text{obs [hemin 3](CN)}_2^{-1}) + \Delta(r - \text{CH}_3) \quad (1)$$

where $\Delta(r - \text{CH}_3)$ is the protein-based perturbation that depends on position r (one of the positions a – h) in Figure 1. The values of $\Delta(r - \text{CH}_3)$ have been determined, in ppm, as $+5.3(a)$, $+2.8(b)$, $-9.9(c)$, $-6.8(d)$, $8.1(e)$, $-10(g)$, and $-4.8(h)$.^{29,43} The results of applying these values to the model compound shifts (Table 1) as a given methyl occupies the four possible positions in the matrix are listed in Table 2 for the four rotational isomers **I**–**IV** depicted in Figure 7. It is clear that the pattern of the shifts, $M_a > M_e > M_f > M_c$ for the major isomer, **I**, is correctly predicted, with the shift values in very reasonable agreement.

We now consider the predicted methyl shifts for the three other possible rotational isomers of metMb(3)CN, those that differ by $\pm 90^\circ$ rotation of the heme normal, as shown for **II** and **IV** in Figure 7, and that which represents a 180° rotation, structure **III** in Figure 7. It is noted in Table 2 that a very different pattern of heme methyl shifts is predicted, depending on the orientation.

Heme Seating in the Minor Isomers. Independent determination of the orientation of the minor isomers requires either the assignment of the heme pocket residue or the location of the three meso-H's for each isomer. However, because the minor isomer peaks are severely broadened by exchange effects even at the lowest temperature, neither the residues nor the meso-H can be located. Moreover, since peaks m_i and m_i^* have comparable intensity, it is not even possible to directly distinguish the four methyls for the two minor isomers, since their intensities are comparable and all but 3 of the 8 methyl signals for the two minor isomers are unresolved. However, such factoring is readily and unambiguously achieved on the basis of the expected heme methyl contact shift pattern^{44–47} in any metMbCN complex. The seating(s) of the minor isomer-

(43) La Mar, G. N.; Emerson, S. D.; Lecomte, J. T. J.; Pande, U.; Smith, K. M.; Craig, G. W.; Kehres, L. A. *J. Am. Chem. Soc.* **1986**, *108*, 5568–5573.

(44) Bertini, I.; Turano, P.; Vila, A. J. *Chem. Rev.* **1993**, *93*, 2833–2933.

(45) Walker, F. A.; Simonis, U. *Biol. Magn. Reson.* **1993**, *12*.

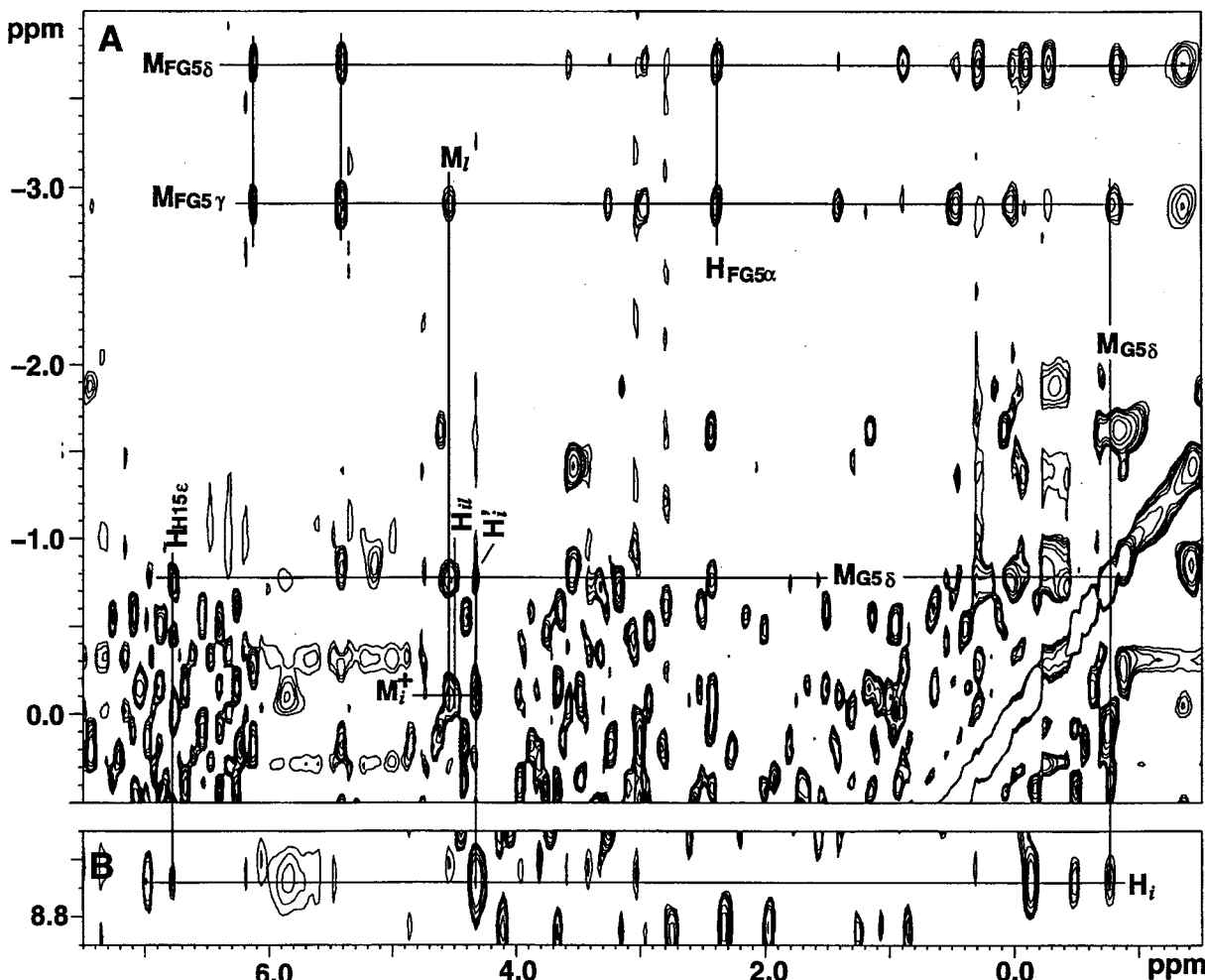


Figure 6. Portions of the 600 MHz ^1H NOESY spectrum (mixing time 60 ms) illustrating the location of the meso-H adjacent to M_i in metMb(3)CN in $^2\text{H}_2\text{O}$, 50 mM phosphate, 100 mM NaCl, 10 mM KCN at pH 8.5 and 20 $^\circ\text{C}$.

(s), moreover, can be determined indirectly from the pattern of the methyl hyperfine shifts.

Thus, the orientation of a N–Fe–N vector relatively close to the projection of the His F8 imidazole plane (see Figure 1) dictates that the porphyrin will exhibit two inversion-related methyls with large shifts that resonate to low-field (30–15 ppm) and two inversion-related methyls with small shifts near the diamagnetic envelope (12–5 ppm).^{44–49} Therefore, the isomers with resolved peaks, m_c , m_i , should have m_i and m_j in the 5–12 ppm window, where only two such peaks, labeled m_i in Figure 4B and m_j in Figure 4C, are observed. Since this isomer *reverses* the relative magnitude of the heme methyl contact shift between inversion related pyrrole pairs, this isomer with peaks m_q must represent a $\pm 90^\circ$ rotation about the heme normal, that is, structure **II** or **IV** in Figure 7.

Distinction between structures **II** and **IV** in Figure 7 for the minor isomer with methyl peaks m_q is readily made on the basis of the *prediction* of the methyl shifts for the two isomers listed in Table 2. Thus, structure **II** correctly predicts the observed

relative methyl shift $M_a > M_c > M_e > M_f$, and hence the isomer with methyls m_q has the nitro group at position *ah*, the canonical δ -meso position. Isomer **IV**, which would place the meso-nitro group at the *de* or canonical β -meso position, predicts (see Table 2) the wrong order for both the strongly and weakly shifted heme methyls, and hence is concluded not to be detectable (<2% population).

Similarly, the two minor species methyl peaks, m^*_i and m^*_j , are observed in the low-field 15–30 ppm window, so that m^*_k and m^*_l are expected to resonate in the 5–12 ppm window, where two such peaks are labeled in Figure 4, D and E, respectively. For this minor isomer, the same pyrrole rings, *i* and *j*, exhibit large contact shifts as observed in the major isomer. This conservation of the contact shift pattern from the major isomer in the minor isomer *demands that this minor isomer differ from the major by a 180° rotation* of meso-NO₂-etioheme I about the heme normal. There is only one such possibility as shown in structure **III** in Figure 7. It is observed in Table 2 that the predicted shifts for structure **III** correlate extremely well with those observed.

Discussion

Molecular/Electronic Structure. The distal and proximal residues for the major isomer **I** (Figure 1) exhibit essentially the same dipolar contacts among each other and with the heme as observed in WT metMbCN,^{25,38} indicating that the heme pocket molecular structure is conserved, as has been found for

(46) La Mar, G. N.; Satterlee, J. D.; de Ropp, J. S. In *The Porphyrin Handbook*; Kadish, K. M., Guillard, R., Smith, K. M., Eds.; Academic Press: San Diego, 1999; Vol. 5, pp 185–298.

(47) Walker, F. A. In *The Porphyrin Handbook*; Kadish, K. M., Guillard, R., Smith, K. M., Eds.; Academic Press: New York, 1999; Vol. 5, pp 81–183.

(48) Shulman, R. G.; Glarum, S. H.; Karplus, M. *J. Mol. Biol.* **1971**, *57*, 93–115.

(49) Shokhirev, N. V.; Walker, F. A. *J. Biol. Inorg. Chem.* **1998**, *3*, 581–594.

Table 2. Chemical Shift of Heme Substituents in the Heme Pocket for the Various Orientations of Meso-nitro-etioheme I Reconstituted into Horse MetMbCN

pyrrole ^b	heme orientation ^a											
	I(0°)			II(+90°)			III(+180°)			IV(+270°)		
	obs ^c	calc ^d	position ^e	obs ^c	calc ^d	position ^e	obs ^c	calc ^d	position ^e	obs ^c	calc ^d	position ^e
M _i	26.75	26	<i>a</i>	11.47	11	<i>c</i>	30.34	30	<i>e</i>		11	<i>g</i>
H _i	8.66		<i>b</i>	—			—					
H _r	4.46		<i>b</i>	—			—					
M ⁺ _i	-0.11		<i>b</i>	—			—					
M _l	4.83	5	<i>c</i>	21.59	22	<i>e</i>	5.91	4	<i>g</i>		19	<i>a</i>
H _l	11.30		<i>d</i>	—			—					
H _r	7.52		<i>d</i>	—			—					
M ⁺ _l	0.32		<i>d</i>	—			—					
M _j	17.70	20	<i>e</i>	5.58	2	<i>g</i>	14.16	17	<i>a</i>		2	<i>c</i>
H _j	13.01		<i>f</i>	—			—					
H _r	7.52		<i>f</i>	—			—					
M ⁺ _j	1.33		<i>f</i>	—			—					
M _k	8.17	8	<i>g</i>	23.18	24	<i>a</i>	9.59	9	<i>c</i>		27	<i>e</i>
H _k	3.49		<i>h</i>	—			—					
H _k	-1.20		<i>h</i>	—			—					
M ⁺ _k	-0.85		<i>h</i>	—			—					
H _{il}	4.69		<i>bc</i>				[NO ₂] ^f		<i>bc</i>		—	
H _{jl}	0.35		<i>de</i>							[NO ₂] ^f		<i>de</i>
H _{jk}	[NO ₂] ^f		<i>fg</i>									
H _{ik}	2.28		<i>ah</i>	[NO ₂] ^f		<i>ah</i>						

^a Heme orientation as defined in Figure 7, with structure I as the reference structure, with the angles of rotation of the other structures II–IV relative to structure I given in parentheses. ^b Core methyls (M_q), core methylene protons (H_q), and terminal methyls (M⁺_q) on the four pyrroles arbitrarily labeled *i*, *j*, *k*, and *l*, and meso-proton, H_{q,q'}, that are at the junction of adjacent pyrroles, as defined in Figures 3 and 4. ^c Observed shifts in ppm, referenced to DSS, in ²H₂O, pH 8.0 at 25 °C. ^d Predicted shift for a given orientation as determined by eq 1 as described in the text. ^e Position of any heme substituent in the myoglobin pocket, as shown in Figure 1. The pyrrole position *a*–*h* correspond to the canonical 1–8 position of native protohemin 1, and meso positions *bc*, *de*, *fg*, and *ah* correspond to the canonical α -, β -, γ -, and δ -meso positions, respectively, of native protohemin 1. ^f The position of the nitro group is indicated by [NO₂].

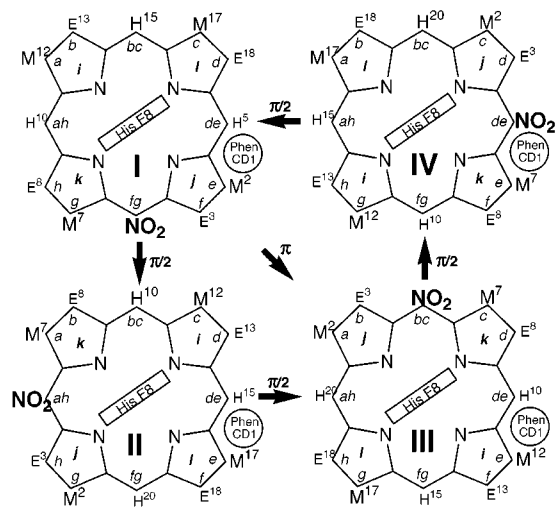


Figure 7. Representation of the four possible isomeric seatings of meso-nitro-etioheme I reconstituted into metMbCN where the orientation of the N–Fe–N vector relative to the His F8 plane is conserved. All labeling symbols are shown simultaneously with *i*, *j*, *k*, *l* representing the individual pyrrole rings as identified by NMR in Figure 4, *a*–*h* the possible pyrrole position, and *bc*, *de*, *fg*, and *ah* the possible meso positions in the pocket of myoglobin (see Figure 1), and the specific position on meso-nitro-etiohemin (as superscript to, M, H) as defined in 3. (I), the nitro group at the canonical γ -meso position, the major (~82%) isomer in solution and the reference for the minor isomers; (II) clockwise rotation by $\pi/2$ to place the nitro group at the canonical δ -position, as determined for the ~8% populated isomer with methyls *m*_q; (III) clockwise rotation by π to place the nitro group at the canonical α -meso position, as found for the 10% populated isomer with methyls, *m*⁺_q; (IV) clockwise rotation by $3\pi/2$ to place the nitro group at the canonical β -meso position; this species is not detected in solution. Note, both the position of the pyrrole rings (*i*–*l*), and the position in the pocket referenced to the protein pocket (*a*–*h*) are shown).

metMbCN complexes reconstituted with other chemically modified hemins.²⁹ Moreover, the chemical shifts, and hence dipolar shifts, for nonligated residues in the heme pocket of the major isomer are very similar to those in WT metMbCN^{25,38} and the complex reconstituted with unreacted etioheme I, 2, (not shown, see Supporting Information).²¹ This requires largely conserved magnetic axes relative to WT whose tilt β reflect the tilt of the Fe–CN unit from the heme normal.^{25,46} The pattern of the heme methyl dominant contact shifts has *trans*-pyrrole rings with similar chemical shifts, as dictated by the orbital hole which allows spin transfer to the pyrroles whose N–Fe–N vector lies approximately normal to the His F8 plane,^{46–49} as observed in all mammalian metMbCN with conserved His F8 ring orientation.⁴⁶ The spacing between the orbital hole ground state and the excited state is comparable to *kT*, as evidenced by the characteristic super-Curie for the pair of strongly shifted, and anti-Curie temperature behaviors for the minimally shifted pair of *trans*-methyls in a Curie plot^{29,44–47,50} (Figure 5).

The minor isomers exhibit slightly different dipolar shifts from those of the major isomer, as evidenced by the resolution of some of the upfield Ile99(FG5) protons (see Ile FG5 C₃H₃ peak labeled by an asterisk in Figure 3A), but the differences are relatively small. The pattern of methyl contact shifts was, in fact, used above to deduce the orientations of the hemin in the pocket. The spacings between the lowest two Kramers doublets⁵⁰ in the minor isomers are similar to that in the major isomer, as evidenced by the super-Curie behavior for the two methyls with large shifts, and anti-Curie behavior for the two methyls with smaller shifts in each case, as illustrated in Figure 5.

Seating of Meso-nitro-etiohemin I. The orientation of meso-nitro etioheme I in horse metMbCN was determined here in complete detail based on the currently accepted protocol for

(50) Brennan, L.; Turner, D. L. *Biochim. Biophys. Acta* **1997**, *1342*, 1–12.

assigning meso-H's shifted by their characteristic temperature behavior and intercept in a Curie plot.⁵¹ However, it is noted that the methyl shift patterns predicted for the four possible isomer seatings of meso-nitroetioheme-I (see Table 2), based on the earlier analysis of numerous metMbCN reconstituted with modified hemins,²⁹ already identify structure **I** in Figure 7 for the major isomer, with methyl contact shifts in the order $M_d > M_e > M_f > M_c$, that is as observed (Table 2). The numerical correlation is also excellent.

The conservation of large contact shifts for methyls *i* and *j* for the isomer with methyl peaks m^*_q alone establishes that the N–Fe–N vector of this species must lie on the same line as the major isomer, and dictates structure **III** in Figure 7. Again, the comparison of observed and predicted shifts provides not only the correct order, but a semiquantitative fit (Table 2). For the case of the isomer with methyl peaks m_q , the methyl contact shift pattern alone provides only the information that the heme has rotated by 90° from that in the major isomer, *but does not indicate in which direction*. The comparison of the observed and predicted shifts (Table 2) for structures **II** and **IV** in Figure 7 clearly distinguishes the two possibilities and identifies structure **II** as the correct isomer. Thus, the present analyses further supports the additivity of rhombic perturbations at individual positions of the heme that are the vector sum of those induced by the peripheral substituent and those exerted by the protein matrix.²⁹ It is expected that this empirical strategy may be essential for determining the heme orientation of any minor isomer involved in rapid dynamic equilibrium with other orientations of the heme.

Steric Access to Meso Positions and Implication for Ring Cleavage by Coupled Oxidation. The heme orientation with the largest population (~82%) has the nitro group at the canonical γ -meso position, and the population indicates that it is ~1.2 kcal/mol more stable than at meso positions α or δ . Interestingly, it was not possible to obtain evidence for detectable population (<2%) of the heme orientation with the nitro group at the canonical β -meso position. This discrimination against the β -meso position is likely due to the very tight interaction¹⁹ between the heme and the ring of the totally invariant Phe43(CD1). A dominant seating at the γ -meso position is, in retrospect, not surprising for at least two reasons. On one hand, the “abbreviation” of the two propionates to a

methyl and ethyl in etiohemin I, **3**, relative to native hemin, **1**, will generate some space in the general vicinity of the γ -meso that is not available in WT Mb. Perhaps more importantly, the nitro group, due to the requirement of out-of-plane orientations of the oxygens,²² is not only bulky, but is also *highly polar*. The heme pocket in Mb is relatively nonpolar except a region near the propionates (i.e., positions *f,g* in Figure 1), which is, in part, exposed to solvent.¹⁹

What is significant is the fact that *the nitro group seats with comparable probability (~10%) at both the hydrophobic canonical α -meso (structure **III** in Figure 7) and δ -meso positions (structure **II** in Figure 7)*. This study clearly demonstrates that, while the static ground-state structure suggests that there is “more space” near the α -meso position in Mb,¹² the flexibility of the heme pocket, in fact, allows the generation of comparable space, at negligible energetic expense, near the δ -meso position. The failure to distinguish between the energetic costs of making space at the hydrophobic α - and δ -meso positions would argue that differential steric access is *not* the prime reason for highly regioselective ring openings of the α -meso position during coupled oxidation of Mb. Recent studies²⁰ of heme cleavage by coupled oxidation in myoglobin mutants had shown that both heme pocket polarity and hydrogen-bonding effects contribute to the stereoselectivity of the cleaved macrocycle. Our results are in accord with their conclusion²⁰ that steric interaction may contribute to, but do not dominate, the stereoselectivity of the ring opening in myoglobin.

Acknowledgment. We are indebted to Anh-T. Tran for valuable assistance in the preparation of apo Mb and its reconstitution. This research was supported by Grants from the National Institutes of Health, GM 26226 (A.L.B., G.N.L.), GM 62830 (G.N.L.) and HL 16087 (G.N.L.). The instruments used in this research were funded, in part, by Grants from the National Institutes of Health RR11973, RR04795, RR08206 and the National Science Foundation, 90-16484.

Supporting Information Available: Four figures (COSY and NOESY spectrum of [hemin **3**](CN)₂⁻¹ and TOCSY and NOESY cross-peaks for heme ethyl groups), and one Table (chemical shifts for heme pocket residues) (PDF). This material is available free of charge via the Internet at <http://pubs.acs.org>.

(51) Qin, J.; La Mar, G. N.; Dou, Y.; Admiraal, S. J.; Ikeda-Saito, M. *J. Biol. Chem.* **1994**, 269, 1083–1090.